Journal of Biomolecular NMR, **20:** 77–82, 2001.
KLUWER/ESCOM

Multiplet component separation for measurement of methyl ^{13}C-^{1}H dipolar couplings in weakly aligned proteins

Georg Kontaxis & Ad Bax
Laboratory of Chemical Physics, National Institute of Diabetes and Digestive and Kidney Diseases, National Institutes of Health, Bethesda, MD 20892-0520, U.S.A.

Received 27 February 2001; Accepted 9 March 2001

Key words: dipolar coupling, IPAP-editing, liquid crystal, methyl group, multiplet editing

Abstract

A simple spectral editing procedure is described that generates separate subspectra for the methyl ^{13}C-{^{1}H$_3$} multiplet components of ^{1}H-^{13}C HSQC spectra. The editing procedure relies on co-addition of in-phase and antiphase spectra and yields ^{1}H-coupled constant-time HSQC subspectra for the methyl region that have the simplicity of the regular decoupled CT-HSQC spectrum. Resulting spectra permit rapid and reliable measurement of ^{1}H-^{13}C J and dipolar couplings. The editing procedure is illustrated for a Ca^{2+}-calmodulin sample in isotropic and liquid crystalline phases.

Following the first measurement by Prestegard and co-workers of ^{1}H-^{15}N one-bond dipolar couplings in myoglobin, weakly aligned with the magnetic field by its paramagnetism (Tolman et al., 1995), such measurements have become widely used. The introduction of dilute liquid crystalline media (Tjandra and Bax, 1997a; Clore et al., 1998; Hansen et al., 1998; Prosser et al., 1998; Barrientos et al., 2000; Fleming et al., 2000; Ruckert and Otting, 2000) and gel-based methods (Sass et al., 2000; Tycko et al., 2000) for inducing tunable degrees of solute alignment has made it possible to measure a wide range of different types of one-bond and more distant dipolar couplings (Tjandra and Bax, 1997a; Ottiger and Bax, 1998; Yang et al., 1999; Tian et al., 2000; Delaglio et al., 2001). These couplings contain information on the orientation of internuclear vectors relative to the alignment tensor of the macromolecule. In contrast to NOE and J couplings, these dipolar restraints are therefore global in nature. Incorporation of dipolar restraints in structure calculations can yield remarkable improvements in quality, both in terms of local geometry and as judged by cross-validation (Tjandra et al., 1997; Cornilescu et al., 1998; Clore et al., 1999; Drohat et al., 1999).

For proteins, most applications so far have focused on the use of backbone dipolar couplings. Several methods for measurement of side-chain dipolar couplings have also been proposed, however. These include the recording of heteronuclear 3D HCCH-type correlation spectra that are ^{13}C-coupled in the ^{1}H dimension (Olejniczak et al., 1999), and a sophisticated E.COSY-type method which permits simultaneous measurement of both individual ^{13}C-^{1}H couplings and the geminal ^{1}H-^{1}H coupling for methylene groups (Carlomagno et al., 2000). A third method measures the $^{1}J_{CH}$ coupling from a set of J_{CH}-modulated constant-time HSQC (CT-HSQC) spectra (Tjandra and Bax, 1997b; Ottiger et al., 1998b), and another recent experiment derives $^{13}C^{\beta}$-$^{1}H^{\beta}$ couplings from the intensity ratios observed in two or three interleaved CB(CA)CONH spectra (Chou and Bax, 2001).

Relatively few measurements have been reported for methyl groups in macromolecules so far. Due to the rapid rotation around their threefold symmetry axis, dipolar couplings are reduced by a factor $P_2(\cos\theta) = (3\cos^2\theta - 1)/2$ relative to a ^{13}C-^{1}H bond that is parallel to the symmetry axis, where θ is the angle between the methyl C-H bond and its symmetry axis. Measurements in proteins indicate that $P_2(\cos\theta)$ for methyl groups is in the -0.31 to -0.33 range (Mittermaier and Kay, 1999; Ottiger and Bax, 1999). These methyl group ^{13}C-^{1}H couplings were simply measured from

HSQC spectra recorded in the absence of ^{1}H decoupling in the ^{13}C dimension. The outer ^{13}C quartet components in such spectra are three times more intense than the inner components and typically yield high sensitivity, which is about 35% of that in the corresponding decoupled CT-HSQC spectrum. Although the methyl group rotation reduces the dipolar coupling by nearly 70%, the outer components of the $^{13}CH_3$ quartet are separated by $3J_{CH}$. The absolute value of the change in splitting for the outer quartet components therefore is less than 10% smaller compared to the dipolar splitting contribution for a single C-H vector oriented parallel to the methyl group axis.

The fourfold increase in the number of resonances that results if ^{1}H decoupling is omitted in the F_1 dimension of CT-HSQC spectra can cause severe spectral crowding. An interesting solution to this problem was presented recently by Kaikkonen and Otting (2001), who proposed to measure the ^{1}H-^{1}H dipolar coupling within the methyl group. Alignment of the methyl group results in a triplet splitting for the protons, where the ^{1}H-^{1}H dipolar coupling causes a separation between the outer components that equals 1.5 times the ^{13}C-^{1}H dipolar contribution to the separation between the outer components of a $^{13}CH_3$ quartet. The precise ratio between ^{1}H-^{1}H and ^{1}H-^{13}C dipolar couplings can reveal interesting information on the methyl group geometry itself (Wooton et al., 1979), but for most protein structural studies the information carried by D_{HH} and D_{CH} couplings is redundant. One potential problem with measurement of D_{HH} couplings is that they are extracted from antiphase ^{1}H multiplets, which can make smaller couplings difficult to measure. Here, we present a spectral editing method that generates CT-HSQC subspectra containing only a single ^{13}C-{$^1H_3$} multiplet component. This method can be considered an extension of the S^{3}E (Meissner et al., 1997) and IPAP-HSQC (Yang and Nagayama, 1996; Ottiger et al., 1998a) methods, which separate heteronuclear doublet components into separate subspectra.

The pulse sequence used for generating $^{13}CH_3$ quartet component subspectra is shown in Figure 1. The scheme is a variant of the original CT-HSQC pulse sequence (Santoro and King, 1992; Vuister and Bax, 1992). It differs by the insertion of a dephasing delay 2Δ, followed by a z-filter, prior to the constant-time t_1 evolution period, which lacks the usual ^{1}H 180° decoupling pulse. Also, in order to minimize the effects of offset and RF inhomogeneity, adiabatic hyperbolic secant inversion pulses (Silver et al., 1984) are used

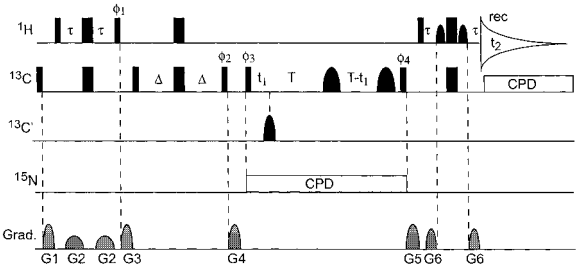

Figure 1. Pulse scheme of the IPAP ^{13}C-$^1H_3$ CT-HSQC experiment. Narrow and wide pulses correspond to 90° and 180° flip angles respectively, with phase x unless indicated. For each t_1 increment, separate data are acquired in an interleaved manner for $2\Delta = 0$, $(6J_{CH})^{-1}$, $(3J_{CH})^{-1}$, and $(2J_{CH})^{-1}$. The low-power, shaped 90° pulses surrounding the final ^{1}H 180° pulse are part of the WATERGATE solvent suppression scheme (Piotto et al., 1992). The ^{1}H 180° pulse at the center of the 2Δ interval is of the composite type (90°_x-210°_y-90°_x). ^{13}C′ and ^{15}N decoupling may be used as indicated, such that correlations for C^α and side-chain Asx and Glx residues are not affected by J_{CC} and J_{CN} couplings. The 180° pulse applied during CT t_1 evolution is of the adiabatic hyperbolic secant variety (375 μs at 201 MHz), with a squareness level of 3 (Silver et al., 1984). Delay durations: $\tau = 1.8$ ms, $2\Delta = 0$, 1.33, 2.67, 4 ms, T = 14 ms. Phase cycling $\phi_1 = 4(y), 4(-y)$; $\phi_2 = x$ for $2\Delta = 0$, $\phi_2 = y$ for $2\Delta = (6J_{CH})^{-1}$, $\phi_2 = -x$ for $2\Delta = (3J_{CH})^{-1}$; $\phi_2 = -y$ for $2\Delta = (2J_{CH})^{-1}$; $\phi_3 = x, -x$; $\phi_4 = 2(x), 2(-x)$; receiver = x,2(−x),x, −x,2(x),−x. Quadrature detection in the t_1 dimension is achieved by alternating ϕ_3 in the usual States-TPPI manner. Gradient durations: $G_{1,2,3,4,5,6} = 4, 1, 3, 3, 3.5, 0.5$ ms; gradient directions: $G_{1,2,3,4,5,6}$ = xy, z, y, z, x, z. All gradients were sine-bell shaped, with peak amplitudes of $G_{1,2,3,4,5,6} = 25, 12, 30, 24, 30, 18$ G/cm.

during the constant-time evolution period, where the second hyperbolic secant pulse serves to remove phase anomalies introduced by the first one (Conolly et al., 1993).

The ^{13}C magnetization vectors at the end of the 2Δ dephasing period are shown in Figure 2. The magnitude of the vectors reflects the signal strength of the components, with the outer ones being three times stronger than the inner components. For $2\Delta = 0$, the resulting spectrum is the same as the regular ^{1}H-coupled CT-HSQC spectrum, with all four multiplet components in-phase (Figure 2A). For $2\Delta = (6J_{CH})^{-1}$, the outer components have refocused and are parallel to the −x axis. The inner components have rotated away from the y-axis by 30°, and only their x component is retained after the subsequent z-filter. The resulting spectrum will therefore yield an antiphase multiplet (Figure 2B) with the center lines being half the magnitude of those in the $2\Delta = 0$ spectrum. Use of $2\Delta = (3J_{CH})^{-1}$ and $2\Delta = (2J_{CH})^{-1}$ yields spectra that have similar antiphase patterns (Figure 2C,D), with the center components in the $2\Delta = (3J_{CH})^{-1}$ spectrum

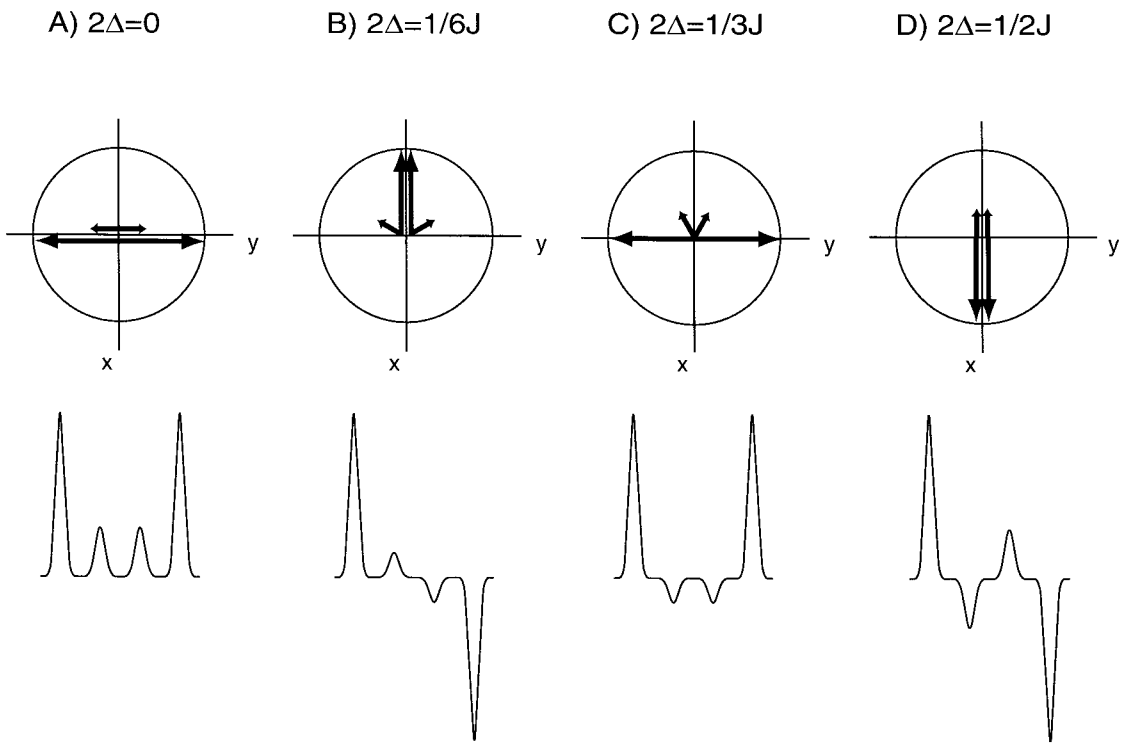

Figure 2. Vector diagram illustrating the evolution of ^{13}C-{H_3} transverse magnetization during the dephasing period 2Δ in the pulse scheme of Figure 1. The vectors correspond to orientations in the xy plane after dephasing delays, 2Δ, of (A) 0, (B) $1/6J_{CH}$, (C) $1/3J_{CH}$, and (D) $1/2J_{CH}$. Underneath each vector diagram the corresponding schematic drawings of F_1 cross-sections through the 2D spectrum for a methyl multiplet are shown. Note that in (B) and (C), where the inner multiplet components have evolved by ±30° and ±60°, only the x (B) and y (C) components are retained after the subsequent z-filter, reducing their amplitude twofold.

again twofold attenuated. The z-filter ensures that the spectra are pure phase, and that undesirable components are purged (Keeler et al., 1994). This z-filter also eliminates ^{13}C-^{13}C double quantum coherence, which results from $^{1}J_{CC}$ dephasing during the 2Δ period, and the subsequent 90° ^{13}C pulse.

If the spectra acquired with $2\Delta = 0$, $2\Delta = (6J_{CH})^{-1}$, $2\Delta = (3J_{CH})^{-1}$ and $2\Delta = (2J_{CH})^{-1}$ are named A, B, C, and D, respectively, linear combinations are taken to select a single multiplet component. For example, as can be readily seen from Figure 2, A + 2B + 2C +D yields only the most downfield multiplet component, whereas A − 2B + 2C − D only retains the most upfield component. Similarly, A + B − C − D only yields the downfield center component, and A − B − C + D yields the upfield center component. For the purpose of measuring dipolar couplings, the outermost quartet components are most useful as they have the highest signal-to-noise ratio, and they also show a threefold larger displacement resulting from dipolar couplings than do the inner components.

For the editing method to be useful, it is necessary that the undesired multiplet components are highly suppressed, such that partial overlap with incompletely canceled components does not affect the apparent peak position of a selected component. In this respect, the editing procedure is highly self-compensating and offers excellent suppression of the undesired components. As a numerical example, we will consider the case where 2Δ is optimized for $J_{CH} = 125$ Hz, and examine the effect of an additional 15 Hz dipolar contribution to the splitting. Note that this coupling is scaled by the methyl group rotation, and corresponds to a dipolar coupling of nearly 50 Hz for a ^{13}C-^{1}H pair oriented in the same direction as the methyl axis. For this case, if the A + 2B + 2C + D spectrum is selected, the center components have spurious intensities of only 3.2% of the selected component, and the upfield component has an intensity that is even weaker (1.4%). So, the editing procedure is quite tolerant to mismatches in the size of the coupling and yields a very high degree of selectivity.

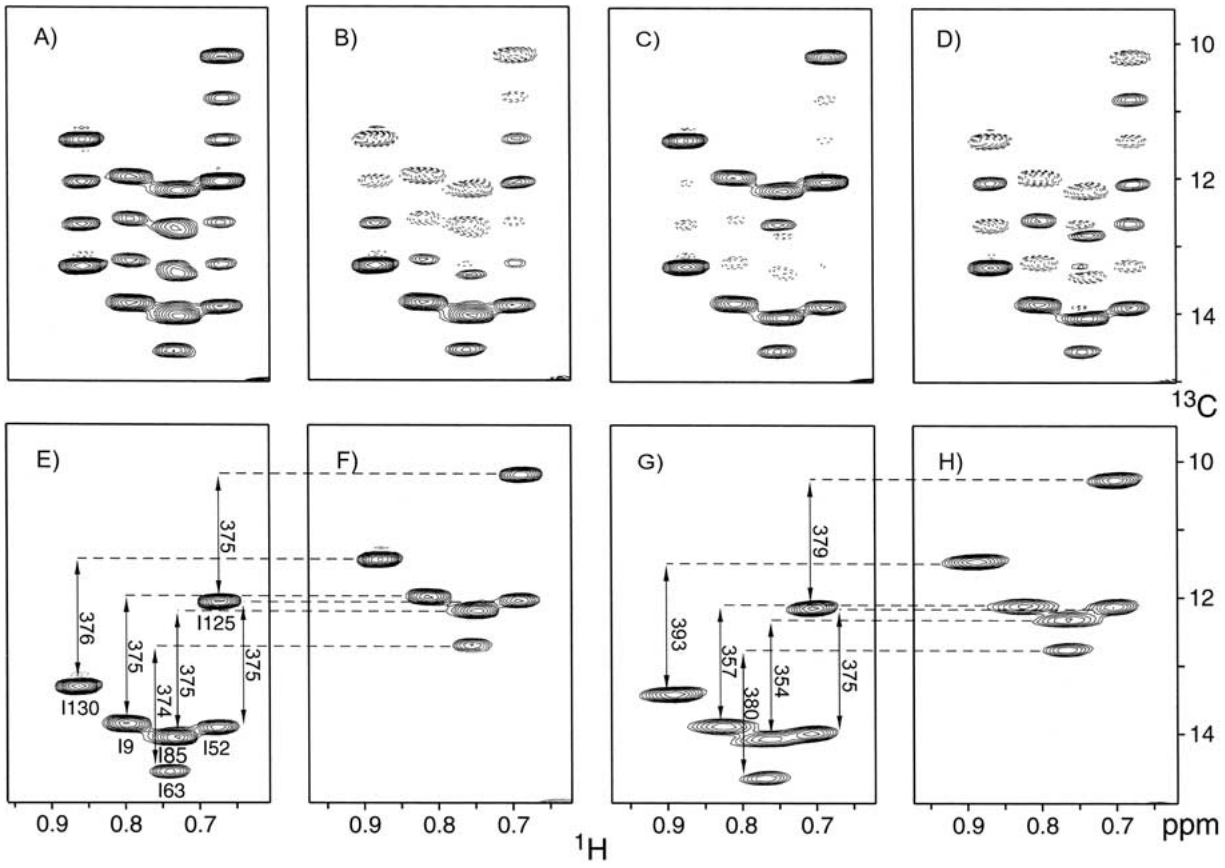

Figure 3. Ile $^{13}C^{\delta 1}$-$^{1}H_3$ region of the IPAP CT-HSQC spectra of Ca^{2+}-ligated calmodulin, recorded at 800 MHz. Panels (A–D) show subspectra for $2\Delta = 0$ (A), $1/6J_{CH}$ (B), $1/3J_{CH}$ (C), and $1/2J_{CH}$ (D), acquired in isotropic solution. Solid and dashed contours mark positive and negative intensity, respectively. Subspectra (E) and (F) result from A + 2.04 B + 2.13 C + 1.14 D and A − 2.04 B + 2.13 C − 1.14 D, respectively. In order to account for T_2 relaxation during the 2Δ intervals, the numerical coefficients differ slightly from those in Equation 1. Assignments are marked in (E), and the displacement between the most downfield and upfield components ($3\ ^{1}J_{CH}$) is also marked. Panels (G) and (H) are the same as (E) and (F), but have been derived from spectra recorded in the liquid crystalline phase. The four interleaved time domain data matrices each consist of $140^* \times 512^*$ data points, with acquisition times of 28 (t_1) and 51 ms (t_2), and 4 transients per FID. The total measuring time for a full set of four spectra was 1.25 h.

From a sensitivity per unit of measuring time perspective, it is optimal if spectra B and C are recorded with twice the number of scans relative to A and D. However, if the subspectra are recorded with identical numbers of transients, the signal-to-noise ratio for a fixed total measuring time is reduced by only a fraction of $1-(3/\sqrt{10})$, i.e., by only 5%. Because signal-to-noise for the methyl region of a CT-HSQC spectrum frequently is not a concern, we recorded all four subspectra with the same minimum number of transients needed for phase cycling, such that the total measurement time was minimized.

Finally, one other point that requires attention is the effect of ^{13}C-^{13}C couplings in uniformly ^{13}C-enriched proteins. The $^{1}J_{CC}$ coupling itself is about 33 ± 1 Hz (Krivdin and Kalabin, 1989), and the dipolar contribution for the above discussed degree of protein alignment equals ±5 Hz. So, the largest possible effective J_{CC} splitting equals 39 Hz, and the smallest possible one equals 27 Hz. The effect of this ^{13}C dephasing is most pronounced for subspectrum D, with $2\Delta = (2J_{CH})^{-1} \approx 4$ ms. ^{13}C-^{13}C dephasing attenuates this spectrum by $\cos(2\pi J_{CC}\Delta)$, which equals 0.882 for $J_{CC} = 39$ Hz, and 0.943 for $J_{CC} = 27$ Hz. This attenuation can largely be compensated for by adjusting the scaling factors used in co-adding the four subspectra to

$$S = A + 2.02 \times B + 2.08 \times C + 1.095 \times D \quad (1)$$

Using these coefficients, the calculated degree of suppression of the non-selected multiplet components

remains better than 99% over the entire range of 27 Hz $< J_{CC} <$ 39 Hz (assuming uniform J_{CH}). The scaling factors in Equation 1 may need to be further adjusted to account for T_2 relaxation during the dephasing period, 2Δ. This can be done by multiplying each subspectrum by its corresponding $\exp(2\Delta/T_2)$ factor, where T_2 is the ^{13}C transverse relaxation time.

The IPAP-CT-HSQC experiment is demonstrated for two samples, containing 0.4 mM $^{15}N/^{13}C$-calmodulin (CaM), pH = 6.5, 100 mM NaCl, 10 mM $CaCl_2$, in the absence and presence of 18 mg/ml Pf1 phage (ASLA Ltd., Riga, Latvia; http://130.237.129.141/asla/asla-phage.html). Both samples were dissolved in ~95% H_2O/5% D_2O in 270 µl thin-wall Shigemi microcells. Experiments were carried out at 32 °C on a Bruker DRX800 spectrometer equipped with a H/N/C triple resonance, three-axis pulsed field gradient probehead. All spectra were processed and analyzed using the NMRPipe software package (Delaglio et al., 1995). Pulse sequence code and processing scripts can be found at http://spin.niddk.nih.gov/bax.

Figures 3A–D show the Ile $^{13}C^{\delta1}$-$^{1}H_3$ regions of the subspectra recorded with the IPAP-CT-HSQC method for the isotropic CaM sample, for 2Δ durations of 0, 1.333, 2.667 and 4 ms. Even in this well-resolved region of the spectrum, partial overlap for four of the six Ile $C^{\delta1}$ resonances occurs, which makes it difficult to measure the corresponding splittings accurately. This overlap is completely removed in Figures 3E and 3F, which show the subspectra for the most downfield and upfield multiplet components, as obtained by linear combination of spectra A–D. For comparison, Figures 3G and 3H show the corresponding regions for the aligned sample. Dipolar contributions to the splittings range from −21 Hz (Ile^{85}) to +17 Hz (Ile^{130}). Outside the region shown, the full range of dipolar contributions to the splitting between the outer quartet components is considerably larger and spans from −32 Hz (Ala^{88}-$C^{\beta}H_3$) to +35 Hz (Val^{91}-$C^{\gamma2}H_3$).

For both the isotropic and liquid crystalline samples, suppression of unselected multiplet components is excellent, even at contour levels much lower than shown in the figure. However, even minute residual peaks resulting from incomplete cancellation can be the source of small peak distortions when partially overlapping a selected multiplet component. We therefore expect that the accuracy of this method is slightly below what can be achieved by the extremely precise J-modulated HSQC method (Tjandra and Bax, 1997b). However, as in liquid crystalline media the range of ^{13}C-^{1}H dipolar couplings usually is quite large, the accuracy attainable in the IPAP-CT-HSQC experiment is more than sufficient for deriving regular structural restraints.

Small changes in the average orientation of a methyl group upon complexation with a target can have a pronounced effect on its dipolar coupling. In addition to simply using methyl group dipolar couplings as restraints in simulated annealing structure calculations, they therefore may also be particularly useful to probe the effect of target binding on a protein surface containing methyl groups. Methyl group dipolar couplings also can provide information on side-chain rotamer distributions, and can yield stereospecific assignments of prochiral Val methyl groups (Chou and Bax, 2001). Several of these applications are currently under investigation.

Acknowledgements

We thank Claude B. Klee and James Chou for sample preparation and useful discussions.

References

Barrientos, L.G., Dolan, C. and Gronenborn, A.M. (2000) *J. Biomol. NMR*, **16**, 329–337.
Carlomagno, T., Peti, W. and Griesinger, C. (2000) *J. Biomol. NMR*, **17**, 99–109.
Chou, J.J. and Bax, A. (2001) *J. Am. Chem. Soc.*, **123**, 3844–3845.
Clore, G.M., Starich, M.R., Bewley, C.A., Cai, M.L. and Kuszewski, J. (1999) *J. Am. Chem. Soc.*, **121**, 6513–6514.
Clore, G.M., Starich, M.R. and Gronenborn, A.M. (1998) *J. Am. Chem. Soc.*, **120**, 10571–10572.
Conolly, S., Nishimura, D. and Macovski, A. (1993) *Magn. Reson. Med.*, **18**, 28–38.
Cornilescu, G., Marquardt, J.L., Ottiger, M. and Bax, A. (1998) *J. Am. Chem. Soc.*, **120**, 6836–6837.
Delaglio, F., Grzesiek, S., Vuister, G.W., Zhu, G., Pfeifer, J. and Bax, A. (1995) *J. Biomol. NMR*, **6**, 277–293.
Delaglio, F., Wu, Z. and Bax, A. (2001) *J. Magn. Reson.*, **149**, 276–281.
Drohat, A.C., Tjandra, N., Baldisseri, D.M. and Weber, D.J. (1999) *Protein Sci.*, **8**, 800–809.
Fleming, K., Gray, D., Prasannan, S. and Matthews, S. (2000) *J. Am. Chem. Soc.*, **122**, 5224–5225.
Hansen, M.R., Mueller, L. and Pardi, A. (1998) *Nat. Struct. Biol.*, **5**, 1065–1074.
Kaikkonen, A. and Otting, G. (2001) *J. Am. Chem. Soc.*, **123**, 1770–1771.
Keeler, J., Clowes, R.T., Davis, A.L. and Laue, E.D. (1994) *Methods Enzymol.*, **239**, 145–207.
Krivdin, L.B. and Kalabin, G.A. (1989) *Prog. NMR Spectrosc.*, **21**, 293–448.

Meissner, A., Duus, J.O. and Sørensen, O.W. (1997) *J. Biomol. NMR*, **10**, 89–94.
Mittermaier, A. and Kay, L.E. (1999) *J. Am. Chem. Soc.*, **121**, 10608–10613.
Olejniczak, E.T., Meadows, R.P., Wang, H., Cai, M.L., Nettesheim, D.G. and Fesik, S.W. (1999) *J. Am. Chem. Soc.*, **121**, 9249–9250.
Ottiger, M. and Bax, A. (1998) *J. Am. Chem. Soc.*, **120**, 12334–12341.
Ottiger, M. and Bax, A. (1999) *J. Am. Chem. Soc.*, **121**, 4690–4695.
Ottiger, M., Delaglio, F. and Bax, A. (1998a) *J. Magn. Reson.*, **131**, 373–378.
Ottiger, M., Delaglio, F., Marquardt, J.L., Tjandra, N. and Bax, A. (1998b) *J. Magn. Reson.*, **134**, 365–369.
Piotto, M., Saudek, V. and Sklenár, V. (1992) *J. Biomol. NMR*, **2**, 661–665.
Prosser, R.S., Losonczi, J.A. and Shiyanovskaya, I.V. (1998) *J. Am. Chem. Soc.*, **120**, 11010–11011.
Ruckert, M. and Otting, G. (2000) *J. Am. Chem. Soc.*, **122**, 7793–7797.
Santoro, J. and King, G.C. (1992) *J. Magn. Reson.*, **97**, 202–207.
Sass, H.-J., Musco, G., Stahl, S.J., Wingfield, P.T. and Grzesiek, S. (2000) *J. Biomol. NMR*, **18**, 303–309.
Silver, M.S., Joseph, R.I. and Hoult, D.I. (1984) *J. Magn. Reson.*, **59**, 347–351.
Tian, F., Fowler, C.A., Zartler, E.R., Jenney, F.A., Adams, M.W. and Prestegard, J.H. (2000) *J. Biomol. NMR*, **18**, 23–31.
Tjandra, N. and Bax, A. (1997a) *Science*, **278**, 1111–1114.
Tjandra, N. and Bax, A. (1997b) *J. Magn. Reson.*, **124**, 512–515.
Tjandra, N., Omichinski, J.G., Gronenborn, A.M., Clore, G.M. and Bax, A. (1997) *Nat. Struct. Biol.*, **4**, 732–738.
Tolman, J.R., Flanagan, J.M., Kennedy, M.A. and Prestegard, J.H. (1995) *Proc. Natl. Acad. Sci. USA*, **92**, 9279–9283.
Tycko, R., Blanco, F.J. and Ishii, Y. (2000) *J. Am. Chem. Soc.*, **122**, 9340–9341.
Vuister, G.W. and Bax, A. (1992) *J. Magn. Reson.*, **98**, 428–435.
Wooton, J.B., Savitsky, G.B., Jacobus, J., Bayerlein, A.L. and Emsley, J.W. (1979) *J. Chem. Phys.*, **70**, 438–442.
Yang, D.W. and Nagayama, K. (1996) *J. Magn. Reson.*, **A118**, 117–121.
Yang, D.W., Venters, R.A., Mueller, G.A., Choy, W.Y. and Kay, L.E. (1999) *J. Biomol. NMR*, **14**, 333–343.